

MOLECULES AT HIGH REDSHIFT: THE EVOLUTION OF THE COOL PHASE OF PROTOGALACTIC DISKS

Colin A. Norman^{1,2} and Marco Spaans¹

Department of Physics and Astronomy, Johns Hopkins University¹ and Space Telescope Science
Institute²

Received _____; accepted _____

ABSTRACT

We study the formation of molecular hydrogen, after the epoch of re-ionization, in the context of canonical galaxy formation theory due to hierarchical clustering. There is an initial epoch of H_2 production in the gas phase through the H^- route which ends at a redshift of order unity. We assume that the fundamental units in the gas phase of protogalaxies during this epoch are similar to diffuse clouds found in our own galaxy and we restrict our attention to protogalactic disks although some of our analysis applies to multi-phase halo gas. Giant molecular clouds are not formed until lower redshifts. Star formation in the protogalactic disks can become self-regulated. The process responsible for the feedback is heating of the gas by the internal stellar radiation field which can dominate the background radiation field at various epochs. If the gas is heated to above $2000 - 3000K$ the hydrogen molecules are collisionally dissociated and we assume that in their absence the star formation process is strongly suppressed due to insufficient cooling. As we demonstrate by analysis of phase diagrams, the H_2 -induced cool phase disappears. *A priori*, the cool phase with molecular hydrogen cooling can only achieve temperatures $\geq 300K$. Consequently, it is possible to define a maximum star formation rate during this epoch. Plausible estimates give a rate of $\lesssim 0.2 - 2M_{\odot}yr^{-1}$ for condensations corresponding to 1σ and 2σ initial density fluctuations. For more massive structures, this limit is relaxed and in agreement with observations of high redshift galaxies. Therefore, the production of metals and dust proceeds slowly in this phase. This moderate epoch is terminated by a phase transition to a cold dense and warm neutral/ionized medium once the metals and dust have increased to a level $Z \approx 0.03 - 0.1Z_{\odot}$. Then: (1) atoms and molecules such as C, O and CO become abundant and cool the gas to below $300K$; (2) the dust abundance has become sufficiently high to allow shielding of the molecular gas and; (3) molecular hydrogen formation can occur rapidly on grain surfaces. This phase transition occurs at a redshift of approximately 1.5, with a fiducial range of

$1.2 \leq z \leq 2$, and initiates the rapid formation of molecular species, giant molecular clouds and stars. The delayed initiation of the cold phase in the interstellar medium of protostellar disks at a metallicity of $Z \lesssim 0.1Z_{\odot}$ is consequently a plausible physical reason that the formation phase of the stellar disks of the bulk of the galaxies only occurs at a redshift of order unity. The combination of feedback and a phase transition provides a natural resolution of the G-dwarf problem.

subject headings: cosmology: theory - galaxies: formation - galaxies: evolution - molecular processes

1. Introduction

Despite numerous searches for molecules at high redshift, the positive results are sparse. The only confirmed observations of molecules at high redshift seen in emission are associated with two gravitational lenses: FSC 10214 + 4724 (Scoville *et al.* 1995, Frayer 1995) and the Cloverleaf (Barvainis *et al.* 1995). In absorption, H_2 has been seen in PKS 0528 - 250 (Foltz *et al.* 1988) at a column density of 10^{18} cm^{-2} , but in no other damped Lyman Alpha system. This is surprising since the column densities of atomic hydrogen inferred for damped Lyman Alpha systems are $\sim 10^{21} \text{ cm}^{-2}$. In comparison with diffuse clouds in our own galaxy such columns seem sufficient to produce H_2 . Galactic diffuse clouds cover the disk with a covering factor between 20–50% where the lower limit is from the Copernicus data (Savage *et al.* 1977) and the upper limit comes from assuming all the infrared Cirrus is associated with diffuse clouds. Other molecular species including HCO^+ , HCN , CO , C^{18}O , HNC , CN , CS and H_2CO have been seen below redshift ~ 1 in the millimeter band (Combes & Wiklind 1996). These absorption techniques are effective for any redshift, provided a bright millimeter continuum background exists. Nevertheless, all the absorbers known to date are in lensed systems with correspondingly small impact parameters.

At lower redshift $z \leq 0.2$ there are well established observations of many molecular species in emission in the nuclei of starburst galaxies (c.f Scoville & Soifer 1991). For large nearby galaxies such as M31 and NGC 891 (c.f. Young 1990) CO maps have been obtained. For our own galaxy, about a hundred different molecular species have been detected in interstellar space. Many di- and tri-atomic molecules can be observed toward diffuse clouds through the visual and millimeter absorption lines they produce in the continua of nearby stars. Some quasars ($\sim 30\%$) used as millimeter calibration sources are known to exhibit absorption lines as well (de Geus *et al.* 1996).

These data pose interesting questions about the prevailing chemical balance and the physical structure of the ambient medium as a function of redshift (c.f. Norman & Braun 1996). Previous work on this subject has focused on very high redshift in the epoch prior to reionization where light-element hydrides such as DH and LiH have been discussed in the context of observations of

deuterium abundances and faint structure in the cosmic background radiation field (Maoli *et al.* 1996, Dalgarno *et al.* 1996, Stancil *et al.* 1996). The importance of H_2 cooling for the formation of the first stars has been discussed by many authors (c.f. Haiman *et al.* 1996, Tegmark *et al.* 1996). Although the self-consistent formation of H_2 above a redshift of $z \sim 6$ due to gas phase processes yields very low abundances of molecular hydrogen $H_2/H \sim 10^{-6}$ (Lepp & Shull 1984), these may be sufficient to sustain the collapse of initial perturbations. In the post re-ionization epoch, the problem of H_2 formation has been discussed by Black *et al.* (1987) for the QSO PHL 957—a damped Lyman Alpha system with an atomic HI column density of $2.5 \times 10^{21} \text{ cm}^{-2}$ —where the H_2 abundance was more than five orders of magnitude lower than values representative of our own galaxy (c.f. Levshakov & Varshalovich 1985, Lanzetta *et al.* 1989). Their analysis indicated that two essential parameters are: (1) the background radiation field which is inferred to be an order of magnitude higher than typical intergalactic values at $z = 2.3$, and (2) the dust-to-gas ratio which is constrained to be no more than $\sim 1/3$ of typical galactic values. Many new results have recently become available on the UV background radiation field (cf. Haardt & Madau 1995), the dust content of damped Lyman Alpha systems (Pettini *et al.* 1994, Fall & Pei 1994) and the merging history of dark matter halos (Kauffmann & White 1993). QSO absorption line studies have also made remarkable progress in the last few years. The high redshift ($z > 2$) dependence of the HI column density distribution function contains valuable information on the early stages of structure formation during which large systems are likely to be in the process of aggregating themselves from smaller sub-units. The obvious candidates to focus on are those systems with HI column densities above $N(HI) \geq 10^{21} \text{ cm}^{-2}$ (Wolfe 1995, Storrie-Lombardi *et al.* 1994). These systems are often associated with protostellar disks and are believed to contain a reasonable fraction of the baryons of the universe.

These new developments motivate us to re-investigate the formation of molecular hydrogen after re-ionization and to assess its role in the standard galaxy formation theory due to hierarchical clustering and the subsequent formation of stars. If the latter process is to occur, a diffuse cool ($T \lesssim 500K$) phase needs to be supported which ultimately leads to the formation of dense molecular clouds and stars. Obviously, the formation of stars produces an internal radiation

field which will heat its surroundings and influence the chemical balance. For star formation to continue, the cool phase should persist. In fact, this process will determine the maximally sustained star formation rate. If the associated time scale is long (comparable to a Hubble time), the abundance of metals and dust will increase slowly until a threshold is reached at which the cooling is dominated by atoms and ions like O and C⁺, as well as molecular species like CO. In addition, H₂ formation on grains proceeds more rapidly and dominates in regions where the bulk of the material is in neutral form. Also, the increased columns of dust absorb the radiation of newly formed stars and sustain a star formation cycle as in our own galaxy. The onset of the bulk of the star formation at low redshifts and moderate metallicity is consistent with current constraints on disk formation. In this paper we have restricted our attention to protogalactic disks since they are the likely sites of the cold molecular phase we are focusing on. Multi-phase halos have been discussed extensively for galaxy formation (c.f. Kang et al 1991, Ikeuchi & Norman 1991) and our results in sections 2.5, 3, 4, and 5 are relevant for such studies although we do not pursue them further here.

This paper is organized as follows. In Section 2, the formation and subsequent evolution of structure in a CDM-dominated Universe is discussed, and the redshift dependence of the UV background radiation field, the stellar radiation field, the gas pressure, the radiation pressure and the ionization parameter are presented. The gas-phase epoch of molecular hydrogen formation is calculated in Section 3 including the production of metals and dust. The feedback effect due to star formation is analyzed in Section 4 and upper limits to the star formation rate and metal and dust production rate are derived. In section 5 we discuss the transition to a multi-phase ISM and the onset of rapid star formation. The epoch when H₂ formation on grains becomes important is discussed in Section 6. The formation of metals and subsequent molecular cooling to massive molecular clouds is also discussed there. Section 7 discusses the implications for the study of the interstellar medium in protogalaxies and star formation, as well as the G-dwarf problem. We associate the onset of star formation in disks with both a redshift, $z \sim 1 - 2$, and a metallicity, $Z \sim 0.03 - 0.1$ as also indicated in a perceptive paper by Wyse and Gilmore (1988). Where possible we give reasonable analytical estimates and then use the full (numerical) details of the

recently calculated metagalactic and stellar radiation fields in our calculations.

2. Basic Cosmological Model

2.1. Galaxy Formation

For the present investigation the specific details of structure formation are of minor importance and we adopt the semi-analytical relations presented by White & Frenk (1991) which agree well with more detailed N-body simulations (cf. Lacy & Cole 1993, 1994; Kauffmann *et al.* 1993, Heyl *et al.* 1995). In the numerical calculations, we also include the merging history of dark matter halos through the conditional probability that a halo of mass M_0 at redshift z_0 has previously been in a halo of mass M_1 at z_1 , as presented in Kauffmann & White (1993).

Using simple top-hat models, the collapse to virial equilibrium of a perturbation that has become non-linear at redshift z results in a density enhancement δ . In CDM scenarios the fiducial value is $\delta = 178$ (Narayan & White 1988). We assume that for protogalactic disks to form, cooling takes place and a fraction of the gas originally contained in the mass perturbation collapses to a centrifugally supported disk with a collapse factor of λ^{-1} , where λ is the spin parameter from tidal torques (cf. Peebles 1993) with a canonical value of $\lambda = 0.07$. Note that there are details of the cooling and infall to the protogalactic disk that we have omitted but they are not essential to the argument given here. For a density perturbation of mass M , the resulting column density is given by

$$N = \left(\frac{4\pi}{3}\right)^{-\frac{1}{3}} \delta^{\frac{2}{3}} \lambda^{-2} \Omega_{b,g} \left(\frac{M}{\mu m_p}\right)^{\frac{1}{3}} n_0^{\frac{2}{3}} (1+z)^2, \quad (1)$$

yielding

$$N = 1 \times 10^{21} \left(\frac{\Omega_{b,g}}{0.01}\right)^{\frac{2}{3}} \left(\frac{M}{5 \times 10^{11} M_\odot}\right)^{\frac{1}{3}} (1+z)^2 \quad \text{cm}^{-2}, \quad (2)$$

with $\Omega_{b,g}$ the baryonic mass fraction in the protogalactic disk relative to the total perturbation.

Our numerical estimates are sensitive to this parameter. In fact, $\Omega_{b,g}$ depends on the merging

history of the dark matter halos and is a function of redshift. Kauffmann (1996, her Figure 12) presents the redshift distribution of the baryonic fraction including the conditional probability for halo merging quoted above. There is a clear maximum between redshift 2 and 3 for a biasing parameter $1 < b < 2$. A value of $b = 1 - 1.5$ seems most consistent with the latest derivations of Storrie-Lombardi & MacMahon (1996). Therefore, we adopt her results in the numerical work presented below.

To characterize the density, we assume that the scale height, H , to disk size, R , denoted by $\eta = H/R$, of the collapsed systems is approximately constant with a typical value of $\eta \sim 1/100$. It follows that the density in the disk is approximately equal to

$$n = \delta \lambda^{-3} \eta^{-1} \Omega_{b,g} n_0 (1+z)^3 \quad (3)$$

yielding

$$n = 5 \left(\frac{100}{\eta} \right) \left(\frac{\Omega_{b,g}}{0.01} \right) (1+z)^3 \quad \text{cm}^{-3}. \quad (4)$$

The canonical mass value is chosen to be $M = 5 \times 10^{11} M_\odot$. Our estimates of the redshift of molecule formation are only weakly dependent on this choice if we focus on the bulk of the matter which is contained in the 1σ and 2σ density perturbations, $M < 10^{12} M_\odot$. We also assume that at high redshift the formation of stars has not been effective in locking up the baryons. The ratio $\psi = (\text{gas/gas} + \text{stars})$ should be of order unity for these proto-galactic objects. Of course, in more evolved systems such as our Galaxy the ratio is only $\sim 10\%$. The actual frequency distribution of objects of mass M is determined by the cosmological model in the context of the Press-Schechter hierarchical clustering picture (c.f. White & Frenk 1991). For a cosmic density parameter $\Omega = 1$, it is assumed here that the total baryonic fraction in galaxies $\Omega_{b,g}$, at a given redshift, cools to a disk while the dark matter remains in the halo. The fraction of baryons in galaxies is typically 10% of the total number of baryons available. The cosmic density of baryons n_{b0} is found to be $n_{b0} = (3H_0^2/8\pi G)(\Omega_b/\mu m_p) = 10^{-6}(\Omega_b/0.1)h^2$, where H_0 is the Hubble constant, $h = H_0/100 \text{ km s}^{-1} \text{ Mpc}^{-1}$, Ω_b is the baryonic fraction of matter in the Universe and μ denotes the reduced mass of the primordial gas for a helium abundance by number of 10%.

The above formulation is for single objects of a given mass and it is therefore worthwhile to formulate a statistical criterium which is more directly related to the initial conditions of structure formation. Equation (1) can also be written as

$$N = n_0 r_0 \delta^{2/3} \lambda^{-2} \Omega_{b,g} (1+z)^2, \quad (5)$$

where r_0 is the initial radius and $r_0 = (3M/4\pi)^{1/3}$. Using the Press-Schechter formalism (see White & Frenk 1991, Equations (1) and (2)), the abundance of halos $n(M, z)$ with mass between M and $M + dM$ is given by

$$n(M, z) = \left(\frac{2}{\pi}\right)^{\frac{1}{2}} \left(\frac{\rho_0}{M^2}\right) y \frac{d \log y}{d \log M} \exp\left(-\frac{y^2}{2}\right) \quad (6)$$

where $y = \delta_c(1+z)/\sigma(M)$, we take $\delta_c = 1.68$ and for standard CDM cosmology $\sigma(M) = 16.3b^{-1}(1 - 0.3909r_0^{0.1} + 0.4814r_0^{0.2})^{-10}$, where r_0 is in units of Mpc and is given by $r_0 = 1(M/10^{12}M_\odot)(\Omega h^2)^{-2/3}Mpc$. The function $\sigma(M)$ can be fitted by an approximate power law $\sigma = \sigma_0(M/M_0)^\alpha$, leading to power law distribution functions $n(M, z) \propto M^{-\alpha-2}(1+z)$ for the halo mass distribution below a characteristic turnover mass defined by $\sigma(M_*(z)) = \delta_c(1+z)$. Gas cooling and resultant disk formation can only occur if the cooling time of the virialized gas in the dark halo at a temperature $T = 2 \times 10^6(M/10^{12}M_\odot)(1+z)K$ is shorter than the dynamical time at a given redshift. This leads to an effective cooling mass as a function of redshift denoted $M_{cool}(z)$. We show in Figure 1 the halo abundance distribution $n(M, z)$. Also shown in the lower $M - z$ plane of Figure 1 are the turnover mass M_* and the limiting mass of the dark halo, M_{cool} , in which there is gas, with $\Omega_{b,h} = 0.05$, that can cool at the given redshift (see also Section 5).

2.2. The Background UV Radiation Field

The background UV radiation field is well approximated for $0.5 < z < 2.5$ by

$$J = J_{-21}(1+z)^{3+q} \quad (7)$$

where J_{-21} is the fiducial value for the intergalactic background in units of $10^{-21} \text{ erg cm}^{-2} \text{ s}^{-1} \text{ sr}^{-1} \text{ Hz}^{-1}$. The value of q lies between $0.5 \leq q \leq 1$, and reflects the uncertainty in the detailed spectral shape of the UV continuum of quasars. Current observations seem to favor a value $q = 0.5$ (Tytler *et al.* 1995). For $z < 3$, Equation (5) is accurate to within 30% over the 912–2000 Å range which is the relevant wavelength region for the H₂ photodissociation process. Above a redshift of three, the quasar population turns over and the metagalactic background decreases with increasing redshift.

In order to more clearly distinguish the effects of H₂ dissociation and ionization heating, the background radiation field is separated into two components, one above and one below the Lyman limit at 912 Å, denoted by $J^>$ and $J^<$, respectively. The actual calculation of the radiation field as a function of both wavelength and redshift requires a numerical integration of the cosmological radiative transfer equation in the absorption line forest (Haardt & Madau 1996). We call this radiation field J_b which is the one used in the numerical computations.

2.3. The Stellar Radiation Field

When star formation is initiated in the protogalaxy, the internally generated radiation field can become significant. For example, at 1000 Å the Draine-Habing estimate for the radiation field in our Galaxy, J_{D-H} , gives an effective radiation field of $J_{-21,D-H} = 30 - 50$. We calculate the luminosity, L_* , and spectral energy distribution for a continuous star formation rate of $1M_{\odot} \text{ yr}^{-1}$, with a Salpeter Initial Mass Function (IMF), and a lower mass cut-off of $1M_{\odot}$ (Leitherer & Heckman 1995). To obtain an intensity, we assume that the stars are being formed uniformly throughout a disk with area A whose nominal value is 100 kpc^2 . In the numerical results we include the more detailed estimates of Kauffmann (1996, her Figures 8 and 13) for the redshift-dependent size of the disk and the radial HI column density distribution. We denote the stellar radiation field by J_* which is given by

$$J_* = L_* \left(\frac{\dot{S}}{A} \right), \quad (8)$$

where \dot{S} is the actual star formation rate. The total radiation field is then

$$J = J_b + J_*. \quad (9)$$

Figure 2 presents the shape and magnitude of the overall radiation field J for various epochs and various star formation rates. For $\dot{S} > 0.02$ the stellar component dominates which strongly increases the intensity in the 912-1110Å region where H₂ is dissociated. The increase is most pronounced for wavelengths longward of the Lyman limit, leading to variations in the relative contributions to $J^<$ and $J^>$.

2.4. Dust and Metallicity Content

The visual extinction to distant QSOs for damped Lyman Alpha systems is not more than a few tenths of a magnitude (Fall & Pei 1994). Fundamental limits have been obtained on the depletion of elements like Zn and Cr in damped Lyman Alpha systems at a redshift of order ~ 3 . Inferred dust-to-gas ratios, ξ_{gd} , are of the order of $\xi_{gd} \sim 0.01 - 0.1\xi_0$ where ξ_0 is the mean galactic value (Pettini *et al.* 1995). The metallicities at these high redshifts are down by approximately the same factor, $Z \sim 1/30Z_\odot$. An accurate analytical model for the redshift dependence of ξ_{gd} and Z is difficult to construct due to the essential role played by star formation. Nevertheless, this dependence should be included since it is a crucial ingredient in our analysis of molecule formation with cosmic epoch. In our numerical work, the metallicity is calculated from the star formation rate in the closed box limit and also in the limit of the ratio of stars to gas being small i.e. $1 - \psi = \text{star}/(\text{star} + \text{gas}) \sim \text{star}/\text{gas} \ll 1$. Consequently we can write

$$Z = \left(\frac{y\dot{S}t}{M} \right) = \left(\frac{2y\dot{S}}{3H_0M} \right) (1+z)^{-\frac{3}{2}}, \quad (10)$$

where $y \approx 0.02$ is the yield of metals like C and O (Woosley & Weaver 1995).

The production of dust follows by assuming that a fraction, ξ_l , of metals is instantly locked up into grains (typically silicate cores). Therefore, we find that the dust-to-gas ratio ξ_{dg} is given by

$$\xi_{dg} = \xi_l Z = \left(\frac{\xi_l y\dot{S}t}{M} \right) = \left(\frac{2\xi_l y\dot{S}}{3H_0M} \right) (1+z)^{-\frac{3}{2}}, \quad (11)$$

As we shall show later, the critical metallicities in our analysis turn out to be $\sim 0.03 - 0.1 Z_{\odot}$. Therefore, we have neglected the significantly lower initial metallicity that may have come from the formation of the halo.

2.5. Gas Pressure, Radiation Pressure and Ionization Parameter

The pressure, P , in the mid-plane of the proto-galactic disk can be estimated by assuming that the mass in the disk is in the gas phase and using the Archimedean formula $P = \rho gh$ where g is the gravitational acceleration normal to the disk. For a thin disk g is given by $g = 2\pi G \Sigma$ where G is Newton's constant and Σ is the surface density of matter in the disk. Therefore, one can write

$$P = 2\pi\mu^2 m_p^2 G N^2, \quad (12)$$

which can be written using equation (1) as

$$P = 2^{-\frac{1}{3}} 3^{-\frac{2}{3}} \pi^{\frac{1}{3}} G \mu^{\frac{4}{3}} m_p^{\frac{4}{3}} \delta^{\frac{4}{3}} \lambda^{-4} \Omega_b M^{\frac{2}{3}} n_0^{\frac{4}{3}} (1+z)^4, \quad (13)$$

with numerical value

$$\tilde{P} = 1200 \left(\frac{\Omega_{b,g}}{0.01} \right)^2 \left(\frac{M}{5 \times 10^{11} M_{\odot}} \right)^{\frac{2}{3}} (1+z)^4 \quad \text{cm}^{-3} \text{K}. \quad (14)$$

where $\tilde{P} = P/k$, and k is Boltzmann's constant. The $(1+z)^4$ dependence of the pressure is slightly misleading due to the essential role played by $\Omega_{b,g}$. In fact, due to the maximum in the redshift dependence of the latter, the sizes of protogalactic disks are smaller at redshifts $z \geq 3$ compared to $z \sim 1$. Note also that at redshift $z \sim 1$, the pressure calculated from the weight of the gas is an order of magnitude greater than the thermal pressure calculated from taking nT . In fact, if one takes the radial dependence of the column density distribution into account and averages over only the inner 3 kpc of the disk, then the gravitational pressure is two orders of magnitude larger than the thermal pressure. This is also the case in our Galaxy and consequently there must be some turbulent pressure that holds up the gas (Boulares & Cox 1990, Norman & Ferrara 1996). The

turbulent pressure is due to kinetic motions from supernovae and superbubbles ultimately due to massive star formation. For low star formation rates the turbulent pressure may not be effective and the mid-plane pressure acting on the thermal component may increase leading to a density increase of more than an order of magnitude. This needs to be kept in mind when discussing the phase diagrams describing the state of the protogalactic gas.

The pressure, \tilde{P}_h , in a virialized halo with a gas fraction $\Omega_{b,h}$ is given by

$$\tilde{P}_h = 80 \left(\frac{M}{5 \times 10^{11} M_\odot} \right)^{\frac{2}{3}} \left(\frac{\Omega_{b,h}}{0.05} \right)^{\frac{4}{3}} (1+z)^2 \quad \text{cm}^{-3}\text{K}. \quad (15)$$

We therefore neglect the halo pressure relative to the disk pressure. More detailed models require the consideration of the pressures and density profiles in the halo and the role of cooling flows to precipitate material from halo to disk. These complex issues will not be addressed further here (c.f. Norman and Meiksin 1996)

The radiation pressure is given by

$$P_{rad} = \frac{4\pi J\nu}{3c}, \quad (16)$$

and we verify that it is always less than the gas pressure in the proto-disks for each of our calculations. We define the ionization parameter used here by $U = J/n$ with n the total number density, and a numerical value defined by $U_{-21} = J_{-21}/n$. The dependence of the pressures and the ionization parameter are shown in Figure 3. The radiation pressure is typically much less than the gas pressure for the epochs studied here, but is of the same order of magnitude for $z \approx 0$. The ionization parameter varies by a factor of five over the $1 < z < 3$ range, because of the turn-over in the quasar population around $z = 2.5$.

3. Gas-Phase Formation of H_2 with Background Radiation

We now turn to examine the epoch when molecular hydrogen is produced in the gas phase. We first use a simple model (Donahue & Shull 1991) to find the approximate analytical expressions

for the molecular hydrogen abundance through the gas phase H^- route.

$$\frac{n(H_2)}{n} = 1.4 \times 10^{-5} T^{0.88} U_{-21} x, \quad (17)$$

where $x = n_e/n$ is the electron abundance and is given by

$$x = 0.02 T^{0.42} U_{-21}^{\frac{1}{2}}. \quad (18)$$

These equations assume that the H^- abundance is in equilibrium and its dominant destruction channel is the reaction with neutral hydrogen yielding H_2 . Conversely, the dominant destruction channels of molecular hydrogen are UV photodissociation and collisional dissociation at temperatures $T > 2500$ K. A simple model for the ionization heating yields

$$T = 3 \times 10^3 U_{-21}^{0.88} n^{0.12}, \quad (19)$$

and the molecular hydrogen abundance is given by

$$\frac{n(H_2)}{n(H)} = 10^{-2} U_{-21}^{0.55} n^{0.14}. \quad (20)$$

For our two component model, where the radiation field is split into a component longward of 912Å and one shortward of the Lyman limit, we find the temperature to be

$$T = 3 \times 10^3 (U_{-21}^{\leq})^{0.27} (U_{-21}^{\geq})^{0.54} n^{0.12} K, \quad (21)$$

and the molecular hydrogen abundance to be equal to

$$\frac{n(H_2)}{n(H)} = 10^{-2} (U_{-21}^{\leq})^{0.85} (U_{-21}^{\geq})^{-0.3} n^{0.15}. \quad (22)$$

In the numerical work, the optically thin H_2 dissociation rate assumed in the above equation has been corrected for the fact that at abundances of the order of 1 column densities in excess of 10^{19} cm^{-2} , H_2 self-shielding plays a role (see below).

4. Gas-Phase Formation of H_2 with Star Formation

4.1. Feedback

It is generally expected that feedback mechanisms may be important in galaxy formation (c.f. Norman & Ikeuchi 1996). The following model is considered here. If the internal star formation generates a dominant radiation field then the gas will be heated to above $2000 - 3000K$ and the molecules will be collisionally dissociated. We assume that the absence of molecular hydrogen formation would strongly limit the efficiency of star formation. From the simple model used above we find that for the stellar radiation field the temperature can be estimated to be

$$T = 7.2 \times 10^3 \left(\frac{\dot{S}}{1M_{\odot} \text{yr}^{-1}} \right)^{0.8} \left(\frac{100 \text{kpc}^2}{A} \right)^{0.8} \left(\frac{n}{1 \text{cm}^{-3}} \right)^{-0.88}, \quad (23)$$

giving a limiting star formation rate of

$$\dot{S}_{crit} = 0.08 \left(\frac{T}{1000K} \right)^{1.25} \left(\frac{n}{1 \text{cm}^{-3}} \right)^{1.1} \left(\frac{A}{100 \text{kpc}^2} \right) M_{\odot} \text{yr}^{-1}. \quad (24)$$

Using the estimate of the density from equation (2) we find that

$$\dot{S}_{crit} = 0.5 \left(\frac{T}{1000K} \right)^{1.25} \left(\frac{100}{\eta} \right)^{1.1} \left(\frac{\Omega_{b,g}}{0.01} \right)^{1.1} \left(\frac{A}{100 \text{kpc}^2} \right) (1+z)^{3.3} M_{\odot} \text{yr}^{-1}. \quad (25)$$

For a Schmidt star formation law where $\dot{S} \propto N^p$ with, $1 < p < 2$, this corresponds to a critical column density

$$N_{crit} = 1 \times 10^{21} \left(0.5 \left(\frac{T}{1000K} \right)^{1.25} \left(\frac{100}{\eta} \right)^{1.1} \left(\frac{\Omega_{b,g}}{0.01} \right)^{1.1} \right)^{\frac{1}{p}} (1+z)^{\frac{3.3-2p}{p}} \text{ cm}^{-2}. \quad (26)$$

For a protogalaxy of a given mass we find that, using the arguments outlined in Section 2, the radius of the disk decreases with redshift as

$$R = 10 \left(\frac{M}{5 \times 10^{11} M_{\odot}} \right)^{\frac{1}{3}} \left(\frac{\Omega_{b,g}}{0.01} \right)^{-\frac{1}{3}} (1+z)^{-1} \text{ kpc} \quad (27)$$

yielding, with $A = \pi R^2$,

$$\dot{S}_{crit} = 1 \left(\frac{T}{1000K} \right)^{1.25} \left(\frac{100}{\eta} \right)^{1.1} \left(\frac{M}{5 \times 10^{11} M_{\odot}} \right)^{\frac{2}{3}} \left(\frac{\Omega_{b,g}}{0.01} \right)^{0.43} (1+z)^{1.3} M_{\odot} \text{yr}^{-1}. \quad (28)$$

For star formation to proceed at all, \dot{S} should be a factor of a few smaller.

4.2. Bursts of Star Formation

We have analyzed the feedback effects in terms of a fixed, continuous star formation rate. We now discuss the burst mode where we envisage the following cycle: the star formation rate is sufficiently high, so that all molecules are dissociated; the star formation turns off; the molecules reform; and another burst occurs.

The time scale, τ_D , for the dissociation of molecular hydrogen, assuming no self-shielding, is

$$\tau_D = 2 \times 10^5 J_{-21}^{-1} \quad \text{yr} \quad (29)$$

and the timescale, τ_F , for the formation of molecular hydrogen is

$$\tau_F = 4 \times 10^8 \left(\frac{1000K}{T} \right)^{\frac{1}{2}} \left(\frac{1cm^{-3}}{n} \right) \quad \text{yr.} \quad (30)$$

Consequently, the duty cycle, $D = (\tau_F/\tau_D)$, of on-burst to off-burst is

$$D = 8 \times 10^{-3} U_{-21} \left(\frac{T}{1000K} \right) \quad (31)$$

Since the amplitude of the radiation field is set by the level of star formation rate it follows that in any burst the mass of the stars formed $M_{*,burst}$ is constant and given by

$$M_{*,burst} = \dot{S} \tau_D \approx 10^6 M_{\odot}. \quad (32)$$

Thus, small bursts can occur but with a very low mean effective star formation rate. It should be emphasized that once a multi-phase medium has been established, bursts can be sustained (Spaans & Norman 1996).

5. The Multi-Phase Structure of the ISM

5.1. Numerical Model

We adopt the heating and cooling curves presented by Donahue & Shull (1991). We include cooling by [OI] 63 μm , [CII] 158 μm and rotational transitions of CO for temperatures below 3000 K. These terms are only of importance for $z < 1.5$. Heating due to photo-electric emission from grains is included and contributes for $z < 1$. At every redshift Equation (9) is used to determine the metallicity and expression (8) yields the ambient radiation field. The latter is integrated over the hydrogen ionization and H_2 photo-dissociation cross sections. The ionization, chemical and thermal balance is solved iteratively until convergence is better than 1% in the temperature and H_2 abundance. The redshift dependence of the baryonic mass fraction is included in the calculation of the column density. In deriving the H_2 abundances we have included the radial $\text{N}(\text{HI})$ profiles of proto-galactic disks as presented by Kauffmann (1996).

5.2. The Moderate Epoch

The results for a fixed star formation rate $\dot{S} = 0.1 M_{\odot} \text{yr}^{-1}$ are presented in Figure 4. Between $z = 4$ and $z = 2$, the gas is kept at a fairly constant temperature of approximately 500 K. This confirms the suggestion by Haiman et al. (1996) that H_2 cooling can facilitate the collapse of high-mass objects and initiate the formation of structure in the early universe. It is also apparent that due to the importance of the stellar radiation field, massive star formation will not occur since a cool phase of $T < 300$ K gas is not present above a redshift of two. In fact, the existence of this moderate epoch ensures that the initial cooling time of the disk is not shorter than the dynamical time at redshifts larger than 3. If this would not be so, then the star formation rates at high redshifts would be much too large.

These effects are further reflected in the abundance of CO which remains low down to a redshift of unity. When the metallicity reaches a threshold of approximately $0.03 Z_{\odot}$, the magnitude of the cooling curve is strongly enhanced. A multi-phase medium is now expected to result. Note that to simplify Equations (10) and (11) for the metal enrichment and dust-to-gas ratio development we have assumed a Schmidt law with index, $p = 1$, implying the star formation

rate per unit mass, \dot{S}/M , is a constant.

5.3. The Phase Transition

Figure 5 presents phase diagrams for various epochs and star formation rates. For early epochs, H_2 is the only coolant below 3000 K and only single temperature solutions exist for certain pressures. As the metallicity increases the $P - n$ curve attains its characteristic S-shape and lines of constant pressure cut it at three different temperatures. That is, a multi-phase medium has formed in which the cool and warm components are stable (Field, Goldsmith & Habing 1969) and which can facilitate large scale star formation. *From Figure 5 one finds that the transition to a multi-phase ISM in the bulk of the galactic disks occurs at $z \approx 1.5$.* At this point it is timely to mention the recent observations of galaxies in the Hubble Deep Field presented by Madau et al. (1996) and Mobasher et al. (1996) for the star formation history of the universe. Although the published results are preliminary, They seem to suggest evidence for a star formation epoch around $z \sim 1 - 2$.

Assuming that there is 1 supernova per $100M_{\odot}$ of stars formed, the filling factor of the hot gas component due to supernovae is (McKee & Ostriker 1977)

$$Q = 0.5E_{51}^{1.28} \left(\frac{\dot{S}}{1M_{\odot} \text{yr}^{-1}} \right) \left(\frac{5 \times 10^{11} M_{\odot}}{M} \right) \left(\frac{0.01}{\Omega_{b,g}} \right) \left(\frac{n}{25 \text{cm}^{-3}} \right)^{1.14} \left(\frac{\tilde{P}}{2.5 \times 10^4 \text{cm}^{-3} \text{K}} \right)^{-1.70} \quad (33)$$

which can be written using the critical star formation rate rate as

$$Q = 0.5E_{51}^{1.28} \left(\frac{5 \times 10^{11} M_{\odot}}{M} \right) \left(\frac{0.01}{\Omega_{b,g}} \right)^{0.14} \left(\frac{\eta}{100} \right)^{1.14} \left(\frac{T}{1000 \text{K}} \right)^{-0.45}. \quad (34)$$

For a Schmidt star formation law, and using Equation (1), we find $Q \propto M^{\epsilon}(1+z)^{-0.38}$ where, $0 < \epsilon < 1/6$, and consequently the estimate is fairly robust.

Therefore, for high star formation rates at the critical value (i.e. more massive objects) the filling factor of hot gas can be significant in these protogalactic disks since the pressure is low and the supernova bubbles can expand and fill large volumes. The above calculation is indicative

only since the star formation is usually clumped and the supernova bubbles generally break out of the disk and vent their energy into the halo of the protogalaxy. This process can also result in a feedback that inhibits star formation (Norman & Ikeuchi 1989). However high star formation rates a multi-phase medium may develop where the hot phase is driven by supernovae energy input. For star formation rates of $0.1 - 0.3 M_{\odot} yr^{-1}$ and below, the hot phase is not significant and a two-phase mode can occur.

6. Formation of H_2 on Grains

An additional important ingredient in the regulation of the star formation is the formation of H_2 on dust grains which renders its abundance independent of the electron fraction. These effects have been included in the models above, but an analytic model is presented here to facilitate a connection with observations.

In the presence of dust and at low densities, molecular hydrogen is formed through grain surface reactions. In steady state, the local H_2 density is given by (Tielens & Hollenbach 1985, van Dishoeck & Black 1986)

$$n(H_2) = \frac{An_H^2}{1 + 2An_H}, \quad (35)$$

where $n_H = n(H) + 2n(H_2)$ is the total hydrogen density. We have discussed the mean density in the disk but it is necessary to make a good estimate of the mean density in the diffuse clouds in the cold neutral medium component where the H_2 formation is most likely to be initiated. We choose to parameterize the clumpiness of the cold neutral clouds by a diffuse cloud covering factor f_c . If, as we have indicated above, the protostellar disks are not subject to substantial massive star formation before molecules are formed then we do not expect the development of a supernova-driven hot ($\sim 10^6 K$) component. Consequently, the temperature and density contrast between the cloud and intercloud component will be modest. We infer that the covering factor of the diffuse cloud component is of order ~ 1 .

The controlling parameter, An_H , is the ratio of the formation rate of molecular hydrogen on grains to the photo-dissociation rate of $H_2.A$ is given by

$$A = \frac{k_s T^{1/2} \xi}{I_{UV} R_{thin} \beta(\tau) e^{-\tau_{UV,C}}}, \quad (36)$$

where I_{UV} denotes the enhancement of the average UV background with respect to the interstellar field at $z = 0$, $\tau_{UV,C}$ is the optical depth in the UV continuum and $\tau_{UV,C} = 2.5 \xi A_V$, R_{thin} is the unattenuated H_2 photodissociation rate and β is the self-shielding function. The rate constant, k_s , depends on the nature of the grains. The value of R_{thin} depends on the precise slope of the UV background between 912 and 1100 Å.

For the present discussion, we want to determine for which epoch molecular hydrogen self-shields in the cold diffuse clouds created in the phase transition, and therefore adopt the constraint

$$A \geq \frac{2}{n_H}, \quad (37)$$

yielding a fractional H_2 abundance of 0.4. For self-shielding, the constraint (37) reduces to

$$I_{UV} R_{thin} \tau_{UV,L}^{-\frac{1}{2}} \exp(-\tau_{UV,C}) \leq \left(\frac{1}{2}\right) k_s T^{1/2} \xi n_H. \quad (38)$$

Explicitly including the redshift dependence and the dependence on covering factor we find that

$$I_{UV,0} R_{thin} f_c^2 \tau_{UV,L,0}^{-\frac{1}{2}} \exp(-\tau_{UV,C,0} f_c^{-1} (1+z)^{\frac{1}{2}}) (1+z)^{\frac{1}{2}+q} \leq \left(\frac{1}{2}\right) k_s T^{1/2} \xi_0 n_{H,0}. \quad (39)$$

Subscripts with zero refer to present time values.

For $\dot{S} \sim 0.03 - 0.1 M_\odot yr^{-1}$ the internally generated radiation field dominates at lower redshifts, $z \sim 1$. In the limiting case where $q = 1$, the total extinction varies slowly with redshift since the lower gas-to-dust ratio of the absorber compensates for its higher column density. In this case, the critical redshift for H_2 formation, z_{mol} , is given by

$$(1+z_{mol}) \leq \left(I_{UV,0}^{-1} R_{thin}^{-1} f_c^{-2} \tau_{UV,L,0}^{\frac{1}{2}} \exp(\tau_{UV,C,0} f_c^{-1}) k_s T^{1/2} \xi_0 n_{H,0} \right)^{\frac{1}{2}}. \quad (40)$$

With a numerical value $z_{mol} = 1.6$.

Including variations in the value of $\dot{S} \sim 0.1 - 0.5$, this yields a fiducial range for H_2 formation of, $1.2 \lesssim z \lesssim 2.0$. These estimates have the advantage that they are weakly dependent on the input parameters. The strongest dependence is on covering factor and star formation rate. Obviously, for small covering factors molecules may form at higher redshift but they will be less observable. Note that the epoch of significant dust shielding and cooling are similar since the dust production and metallicity production are closely related.

The increasing dust columns can absorb a significant fraction of the internal stellar radiation field and this will influence the the time scale on which subsequent star formation proceeds. Using the formalism of McKee (1983) it is possible to estimate the effect of the dust column on the star formation rate. There is a critical extinction of approximate 4 mag, necessary to absorb most of the radiation of newly formed stars. The time scale to convert all available mass into stars for a density of roughly 1000 cm^{-3} is given by

$$3.2 \times 10^7 \xi \left(\frac{1}{2\xi^2} \right)^{0.5+1.25/A_V} \left[\left(1 + \frac{1}{8\xi^2} \right)^{0.5} + \left(\frac{1}{8\xi^2} \right)^{0.5} \right]^{1-2.5/A_V} e^{16/A_V} \text{ yr} \quad (41)$$

and the dust extinction $A_V = 4\xi(1+z)^2$. For $z > 2$ this time scale is much larger than the local Hubble time, but for epochs later than 1.7 star formation can proceed efficiently in the bulk of the galaxies.

6.1. Statistical Approach

The covering factor discussed above is ultimately determined by the process of galaxy formation. Using the statistical approach discussed in Section 2, for any given redshift, the condition (37) for H_2 formation on grains can be written as

$$r_0 > r_{0,\text{crit}}(z). \quad (42)$$

The fraction of galaxies which contain molecules, $f_{\text{mol}}(z)$, is then given by

$$f_{\text{mol}}(z) = \frac{\int_{\ell(r_{0,\text{crit}}(z),z)}^{\infty} e^{-x^2} dx}{\int_{\ell(0,z)}^{\infty} e^{-x^2} dx}, \quad (43)$$

where $\ell(r_0, z) = \left(\frac{\delta_c(1+z)}{2^{1/2}\sigma(r_0)} \right)$. The definition of the statistical epoch of molecule formation is taken to be $f_{\text{mol}}(z) \approx 0.5$. Inversion of this condition yields $\langle z_{\text{mol}} \rangle$. For the parameter values adopted above and putting the biasing parameter $b = 1$, the relations $r_{0,\text{crit}} = 0.17(1+z)^{2+2\alpha}$ Mpc and $\langle z_{\text{mol}} \rangle = 1.5$ approximately hold. Note that $r_{0,\text{crit}}$ does not depend on biasing, but the value of $\langle z_{\text{mol}} \rangle$ does.

Finally, the probability, \mathcal{P} , that a given line of sight to a QSO will show molecular absorption by an intervening damped Lyman Alpha cloud in a (proto-)galaxy is given by (Peebles 1993)

$$\mathcal{P} \approx \int \sigma n_0 c H_0^{-1} \Omega_b^{-1/2} (1+z)^{1/2} dz, \quad (44)$$

where the integral extends over redshifts between 0 and $\langle z_{\text{mol}} \rangle$ and $\sigma = \pi r_g^2$. The characteristic radius (bright part) of the galaxy is chosen equal to $r_g = 10h^{-1}$ kpc. With the parameters given above this yields $\mathcal{P} \approx 8 \times 10^{-2}$.

Once the conditions are satisfied for molecular hydrogen formation the time scale is of order $\sim 1/(n_H \xi) Gyr \sim 10^8(1+z)^{-(p+1)} yr$. The ion-chemistry proceeds much faster on a time scale of approximately $3 \times 10^3(1+z)^{-6} yr$. Thus, once the hydrogen molecules can be formed on grains, the full range of diffuse cloud species follows immediately.

7. Conclusions, Discussion and Implications

Initially motivated by QSO absorption-line observations indicating an absence of molecular hydrogen at high redshift, we have examined the formation of molecular hydrogen, after the epoch of re-ionization, in the context of canonical galaxy formation theory due to hierarchical clustering. The issue of molecular hydrogen at high redshift has been discussed in recent interesting papers by Haiman *et al.* (1996) and Tegmark *et al.* (1996). Whereas they concentrated more on the redshifts above $z \gtrsim 10$, we are focusing on the physics of the phases of the protogalactic gas at redshifts $z \sim 1 - 10$. We have been able to use recently computed accurate models for the cosmic background radiation field (Haardt & Madau 1996) and for the radiation field from a stellar

population with a Salpeter IMF and with a $1M_{\odot}$ lower-mass cut-off in a continuous star forming mode (Leitherer & Heckman 1995). We have also used a simple model for a protogalactic disk and followed conventional CDM cosmology extended by more recent numerical calculations when considering the spectrum of disk masses and column densities. We have mainly concentrated on structures associated with 1σ and 2σ density fluctuations which are expected to form the bulk of the stars.

As with the recent work by Haiman *et al.* (1996) and Tegmark *et al.* (1996) we find there is an initial epoch of H_2 production in the gas phase produced through the H^- channel route where the abundance of molecular hydrogen is approximately 1% and given simply in terms of the ionization parameter by equations (20) and (22). Predicting the details of the state of the interstellar medium of protogalaxies is a complex task. We have normalized to what is known from work on the neutral phase of our Galaxy and assume that the fundamental units in the gas phase of protogalaxies during this epoch are akin to the diffuse clouds found in our own galaxy. We have shown that until the metallicity of the gas achieves $Z \sim 0.03 - 0.1$ at a redshift of 1-2, cold giant molecular clouds are not formed due to inefficient cooling. We have found that star formation in the protogalaxies can become self-regulated due to heating of the gas by the internal stellar radiation field. We have given a simple analytic model for the feedback process in Section 4.1. It is possible to define a maximum star formation rate during this epoch. Plausible estimates give a rate of $\lesssim 1M_{\odot} \text{yr}^{-1}$ and therefore we have considered an appropriate fiducial star formation rate to be $\sim 0.1 - 0.3M_{\odot} \text{yr}^{-1}$. The production of metals and dust proceeds slowly in this self-regulated mode. This slow star formation phase was shown to terminate once the metal abundance increased to a level of approximately $Z \sim 0.03 - 0.1Z_{\odot}$. From an analysis of the phase diagrams in Figure 5, we found that species such as C, O and CO become sufficiently abundant and can cool the gas below $300K$ to $\sim 10 - 30K$. At this point a phase transition can occur in the protogalactic gas. For the low fiducial star formation rates discussed above, we find this to be a transition to a two-phase medium as described by Field, Goldsmith & Habing (1969). Dense molecular clouds can form and the star formation is no longer self-regulated in the manner described above since the UV radiation does not penetrate the dense cores of the clouds. We

expect that rapid, massive star formation ensues and the abundance of metals and dust increase concomitantly. The dust abundance also becomes sufficiently high to allow molecular hydrogen formation on grain surfaces. With the increased star formation rates, the ISM will change to one dominated by supernovae energy input (McKee & Ostriker 1977) with significant exchange of mass, energy and metallicity from the disk to the halo (Norman & Ikeuchi 1989). In a subsequent paper we will investigate in more detail the effects of this phase transition on the evolution of dwarf galaxies and the importance of metal loss driven by supernova explosions.

Our analysis may be of relevance to the G-dwarf problem: the Simple model (Pagel 1989, and references therein) for chemical enrichment overproduces the number of metal-poor stars (Cowley 1995; Worthey, Dorman & Jones 1996 and references therein). Of the many solutions proposed for the G-dwarf problem, the simplest appears to be that by the time a few percent of the gas mass of a galaxy is assembled into stars, the remaining gas reservoir is already enriched in metals and has not yet experienced any star formation. The moderate phase due to feedback identified in this work, is likely to cause star formation in an inhomogeneous way. The very nature of the feedback mechanism dictates that star formation in one location strongly suppresses additional star formation in its vicinity. The subsequent phase transition then causes rapid star formation throughout the mostly unprocessed ISM which now has a metallicity close to 10% of solar.

In our analysis we have assumed a fixed value for the collapse factor λ^{-1} . In reality, the distribution of spin parameters may be quite wide (Warren et al. 1992; Dubinsky & Carlberg 1991). If we view the disk as being formed from a spherical object sustaining a low H_2 abundance, driven by the extragalactic UV background, then an increase in the collapse factor will increase the total and H_2 column densities quadratically and the local density like λ^3 . Consequently, more of the stellar radiation can be absorbed locally, preserving the H_2 abundance and suppressing the global heating, and a higher star formation rate can be sustained. We estimate, although tentatively, that for objects with $\lambda \sim 0.02$, a factor of 3.5 below our canonical value, the redshift at which the phase transition occurs, can be as high as three. More detailed knowledge of the λ distribution is necessary to assess how common such high redshift objects are.

In summary, from our elementary cosmological model we conclude that this new mode of star formation, where objects now akin to giant molecular clouds in our Galaxy become the sites of star formation, occurs at a redshift of approximately 1.5 with a value higher by a factor of 2 if more massive initial perturbations or larger collapse factors are considered. The phase transition in the interstellar medium of protogalactic disks as analyzed in this paper is now a plausible physical reason that the formation of disks of galaxies occurs at a redshift of order unity with a significant increase in star formation after the metallicity has achieved a value of order $Z \sim 0.03 - 0.1 Z_{\odot}$. These findings are consistent with the recent studies of the Hubble Deep Field (cf. Madau et al. 1996; Mobasher et al. 1996). The combination of feedback and a phase transition can provide a natural solution to the G-dwarf problem.

We are grateful to Tim Heckman, David Neufeld and Rosemary Wyse for illuminating and stimulating discussions that contributed significantly to our understanding, and to Andrea Ferrara, Claus Leitherer and Piero Madau for such discussions and also for providing us with their excellent data on low-metallicity cooling curves, the spectrum of radiation from stellar populations and the cosmic background radiation field. We are also grateful to Piero Rosati for his assistance in the presentation of the numerical results. We thank the anonymous referee for his detailed and valuable comments. MS also acknowledges with gratitude the support of NASA grant NAGW-3147 from the Long Term Space Astrophysics Research Program.

REFERENCES

Barvainis, R., Tacconi, L., Antonucci, R., Alloin, D. Maloney, P. & Coleman, P. 1996, in preparation

Black, J.H., Chaffee, F.H. & Foltz, C.B., 1987, *ApJ* 317, 442

Black, J.H. & Dalgarno, A., 1977, *ApJS* 34, 405

Boulares, A. & Cox, D.P. 1990, *ApJ* 365, 444

Combes, F. & Wiklind, T. 1996, in Proceedings of Cold Gas at High Redshift, August 28-30, 1995, eds. P.van der Werf and H. Rottgering (Kluwer), in press

Cowley, C.R., 1995, An Introduction to Cosmochemistry (Cambridge)

Dalgarno, A., Kirby, K. & Stancil, P.C., 1996, *ApJL* 458, L397

de Geus, E.J., Hogerheijde, M.R. & Spaans, M., 1996, *A&A*, submitted

Donahue, M. & Shull, J. M. 1991, *ApJ* 383, 511

Dubinsky, J., Carlberg, R.G., 1991, *ApJ* 378, 496

Fall, S.M. & Pei, Y.C.C., 1993, *ApJ* 402, 479

Field, G.B., Goldsmith, D. & Habing, H.J. 1969, *ApJ* 155, L149

Foltz, C.B., Chaffee, F.H. & Black, J.H., 1988, *ApJ* 324, 267

Frayer, D. 1995, PhD Thesis, University of Virginia.

Haardt, F. & Madau, P., 1996, *ApJ* 461, 20

Haiman, Z., Rees, M.J. & Loeb, A. 1996, *ApJ* 467, 522

Haiman, Z., Thoul, A. & Loeb, A. 1996, *ApJ* 464, 523

Heyl, J.S., Cole, S. Frenk, C.S. & Navarro, J.F., 1995, *MNRAS* 274, 755

Ikeuchi, S. & Norman, C. 1991, *ApJ* 375, 479

Kang, H., Shapiro, P., Fall, S. M. & Rees, M.J. *ApJ* 363, 488

Kauffmann, G., White, S.D.M., 1993, MNRAS 261, 921

Kauffmann, G., Guiderdoni, B. & White, S.D.M., 1994, MNRAS 267, 981

Kauffmann, G., 1996, MNRAS 281, 475

Lacy, C., Cole, S., 1993, MNRAS 262, 627

Lacy, C., Cole, S., 1994, MNRAS 271, 676

Lanzetta, K.M., Wolfe, A. M. & Turnshek, D.A., 1989, ApJ 344, 277

Leitherer, C. & Heckman, T. 1995, ApJS 96, 9

Lepp, S. & Shull, J.M., 1984, ApJ 280, 465

Levshakov, S.A. & Varshalovich, D.A., 1985, MNRAS 212, 517

Madau, P., Ferguson, H.C., Dickinson, M.E., Giavalisco, M., Steidel, C.C., Fruchter, A., 1996, MNRAS, in press

Maoli, R., Ferrucci, V., Melchiorri, F., Signore, M., 1996, ApJ 457, 1

McKee, C.F. 1989, ApJ 345, 782

McKee, C.F. & Ostriker, J.P. 1977, ApJ 218, 148

Mobasher, B., Rowan-Robinson, M., Georgakakis, A., Eaton, N., 1996, MNRAS 282, L7

Narayan, R. & White, S.D.M., 1988, MNRAS 231, 97p

Norman, C. & Braun, R. 1995 in Proceedings of Cold Gas at High Redshift, August 28-30, 1995, eds. P. van der Werf and H. Rottgering (Kluwer), in press

Norman, C. & Ferrara, A. 1996, ApJ 467, 280

Norman, C. A. & Ikeuchi, S. 1989, ApJ 345, 372

Norman, C. A. & Ikeuchi, S. 1996, ApJ, in preparation

Norman, C. A. & Meiksin, A. 1996, ApJ 468, 97

Pagel, B.E.J., 1989, in Evolutionary Phenomena in Galaxies, eds. J. Beckman & B.E.J. Pagel (Cambridge)

Peebles, P.J.E., 1993 *Principles of Physical Cosmology* (Princeton: PUP)

Pettini, M., Smith, L.J., Hunstead, R.W. & King, D.L., 1994, *ApJ* 426, 79

Savage, B.D., Bohlin, R.C., Drake, J.F. & Budich, W., 1977, *ApJ* 216, 291

Scoville, N.Z. & Soifer, B.T. 1991 in *Massive Stars in Starbursts* STScI Symposium Series 5, ed. C. Leitherer, N. Walborn, T. Heckman and C. Norman, p. 233 (Cambridge: CUP)

Scoville, N.Z., Yun, M.S., Brown, R.L. & Vanden Bout, P.A., 1995, *ApJ* 449, L 109

Spaans, M., Norman, C.A., 1996, *ApJ*, submitted

Stancil, P.C., Lepp, S. & Dalgarno, A., 1996, *ApJ* 458, 401

Storrie-Lombardi, L.J., McMahon, R.G., Irwin, M.J. & Hazard, C., 1994, *ApJ* 427, L13

Storrie-Lombardi, L.J., MacMahon, R.G., 1996, preprint

Tegmark, M., Silk, J. Rees, M.J., Blanchard, A., Abel, A. & Palla, F., 1996, *ApJ*, in press

Tielens, A.G.G.M & Hollenbach, D.J. 1985, *ApJ* 291, 722

van Dishoeck, E.F. & Black, J.H., 1986, *ApJS* 62, 109

Warren, M.S., Quinn, P.J., Salmon, J.K., Zurek, W.H., 1992, *ApJ* 399, 405

White, S.D.M & Frenk, C.S., 1991, *ApJ* 379, 52

Wolfe, A. M. 1995 in *QSO Absorption Lines*, ESO AStrophysics Symposia, ed. G. Meylan, p.13 (Berlin: Springer)

Woosley, S. E. & Weaver, T. A. 1995, *ApJS* 101, 181

Worthey, G., Dorman, B., Jones, L.A., 1996, *AJ* 112, 948

Wyse, R. F. G. & Gilmore, G. 1988, *AJ* 95, 1404

Young, J. 1990 in *The Interstellar Medium in Galaxies* Astrophysics and Space Science Library 161, ed. H. Thronson & M. Shull, p. 67 (Dordrecht: Kluwer)

Fig. 1.— Figure 1 shows the abundance of halos as a function of mass and redshift for standard CDM with biasing parameter $b = 1$. The lower $M - z$ plane shows, as functions of redshift, the characteristic turnover mass, M_* (solid curve), in CDM and the limiting mass of the dark halo, M_{cool} (dashed curve), in which gas can cool.

Fig. 2.— Figure 2 shows the combined stellar and background radiation fields at redshift $z = 1$, 2.5, and 4 for star formation rates of 0.01, 0.1 and $1M_{\odot}yr^{-1}$. For rates larger than 0.03 the stellar component dominates and feedback is important.

Fig. 3.— Figure 3 shows the derived gas pressure, radiation pressure and ionization parameter as functions of redshift for $\dot{S} = 0.1M_{\odot}yr^{-1}$. The radiation pressure is typically much less than the gas pressure due to the low star formation rate at which the feedback mechanism is most efficient.

Fig. 4.— Figure 4 shows the results of the calculations for the gas temperature and the abundance of molecular hydrogen, CO, dust (ξ_{gd}), and metals (Z_m) as functions of redshift for a star formation rate $\dot{S} = 0.1M_{\odot}yr^{-1}$.

Fig. 5.— Figure 5 shows pressure, P , and gas density, n_H , phase diagrams for redshifts 1, 2 and 3, respectively and star formation rates of 0.01, 0.1 and $1M_{\odot}yr^{-1}$. The curve in the upper left panel denotes constant pressure. The symbol Z indicates the metallicity with respect to galactic at that epoch for a particular star formation rate. The labels F, G and H denote the thermal equilibria of which G is unstable.

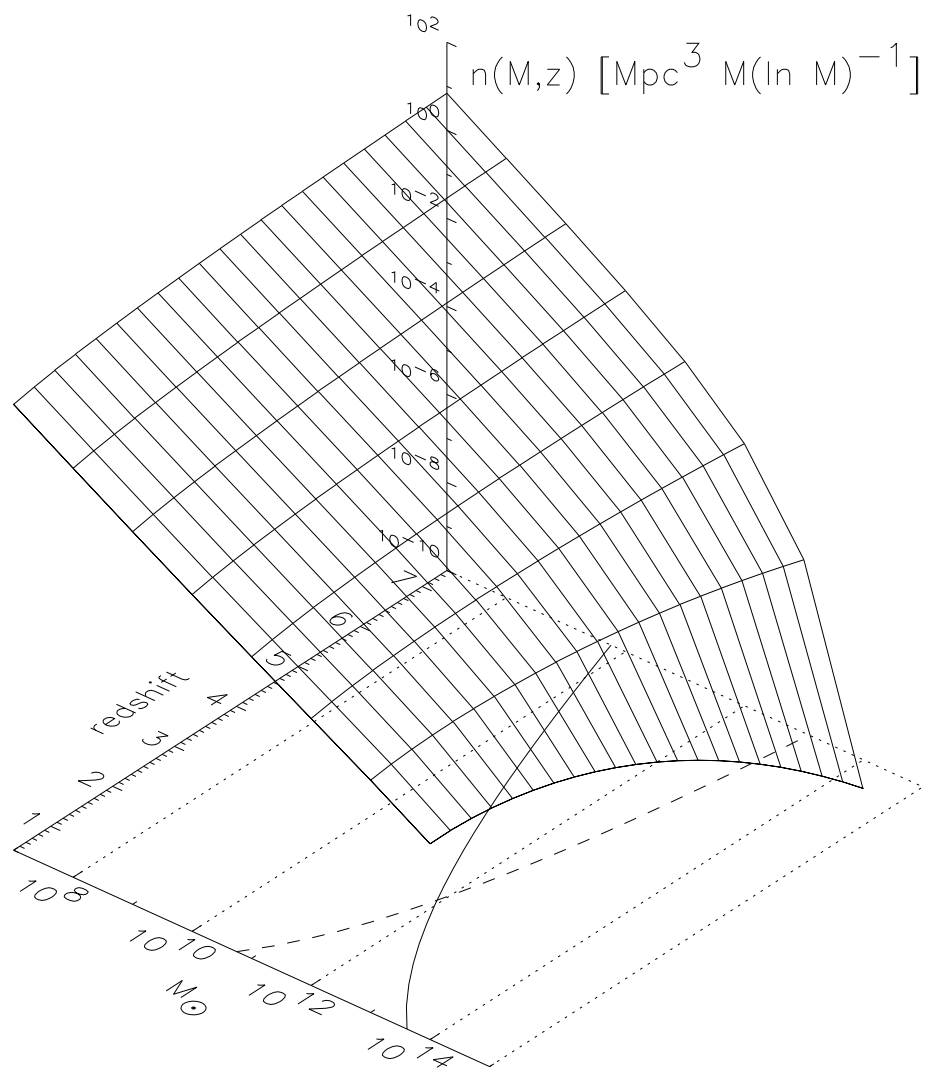


Fig. 1.—

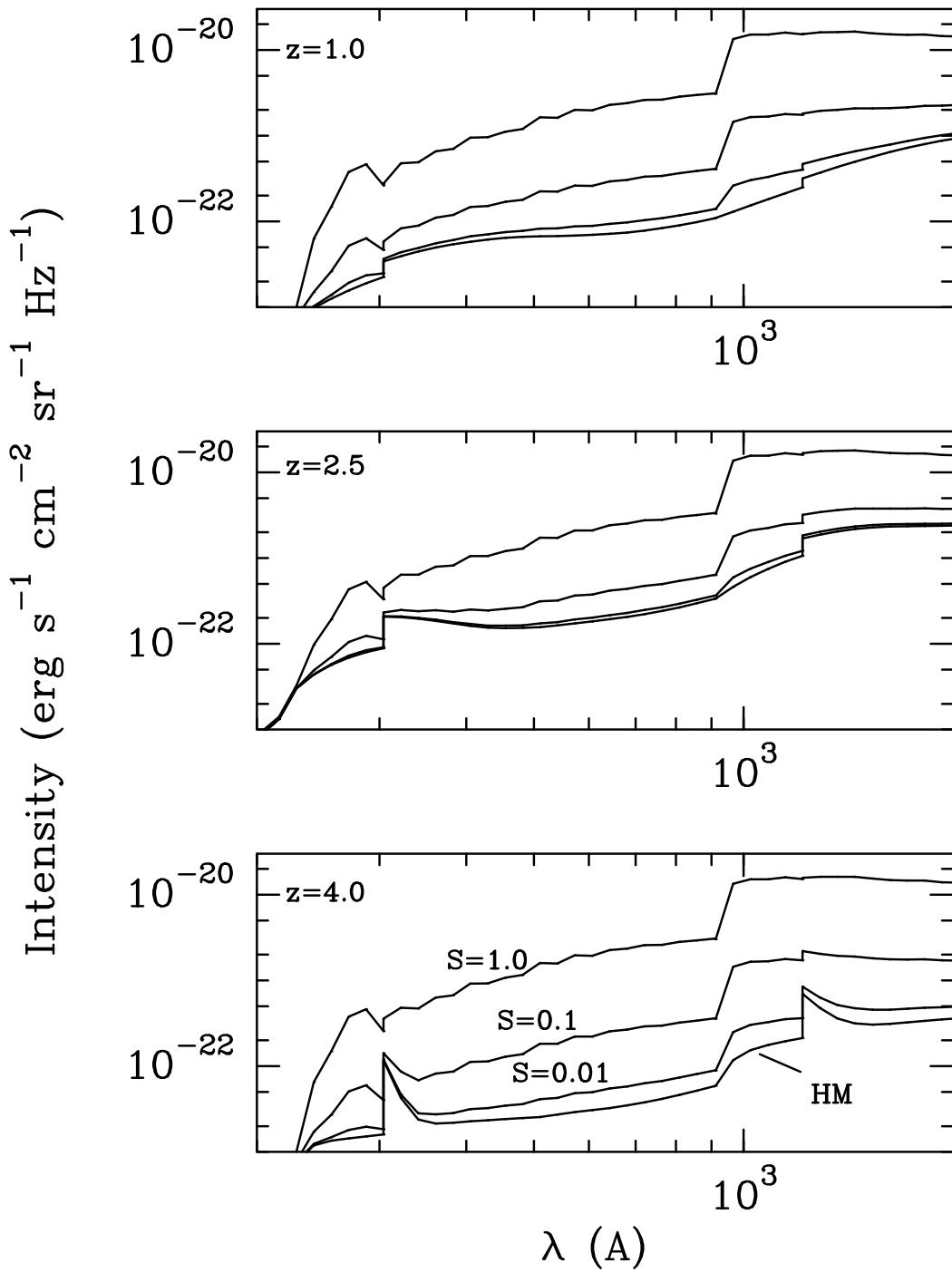
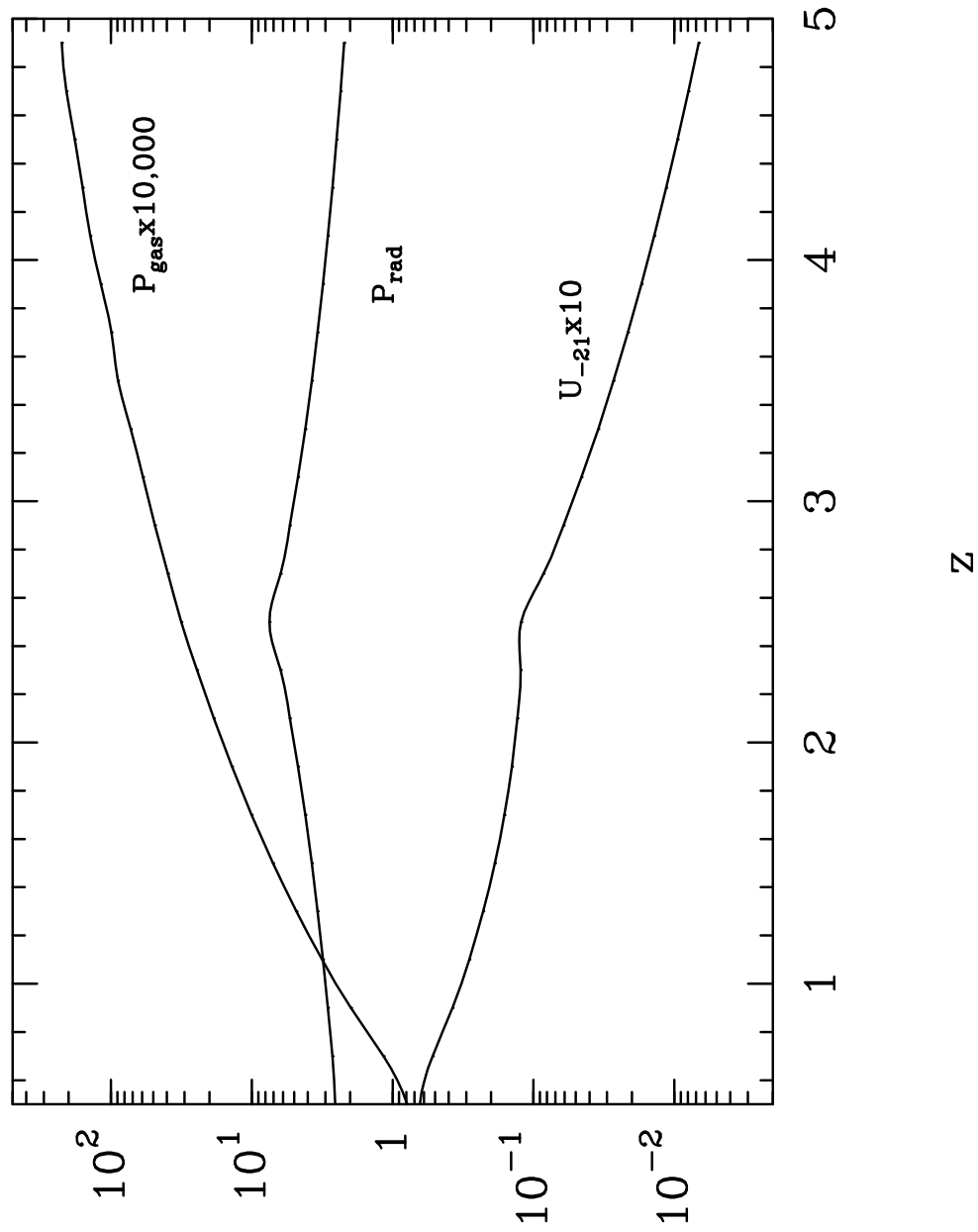


Fig. 2.—



$$P_{\text{gas}} \text{ (Kcm}^{-3}\text{)}, P_{\text{rad}} \text{ (Kcm}^{-3}\text{)}, U_z \text{ (cm}^{-3}\text{)}$$

Fig. 3.—

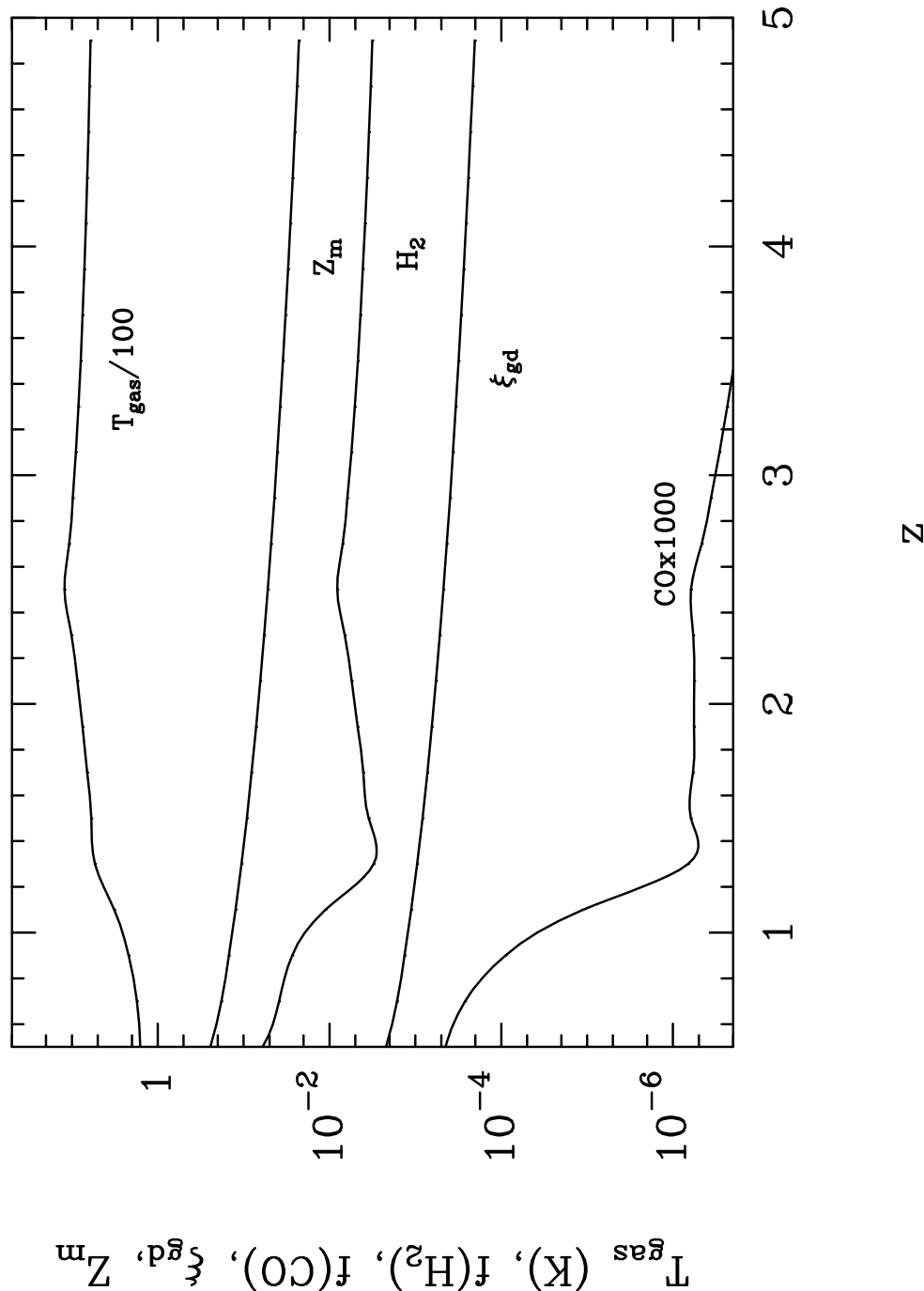


Fig. 4.—

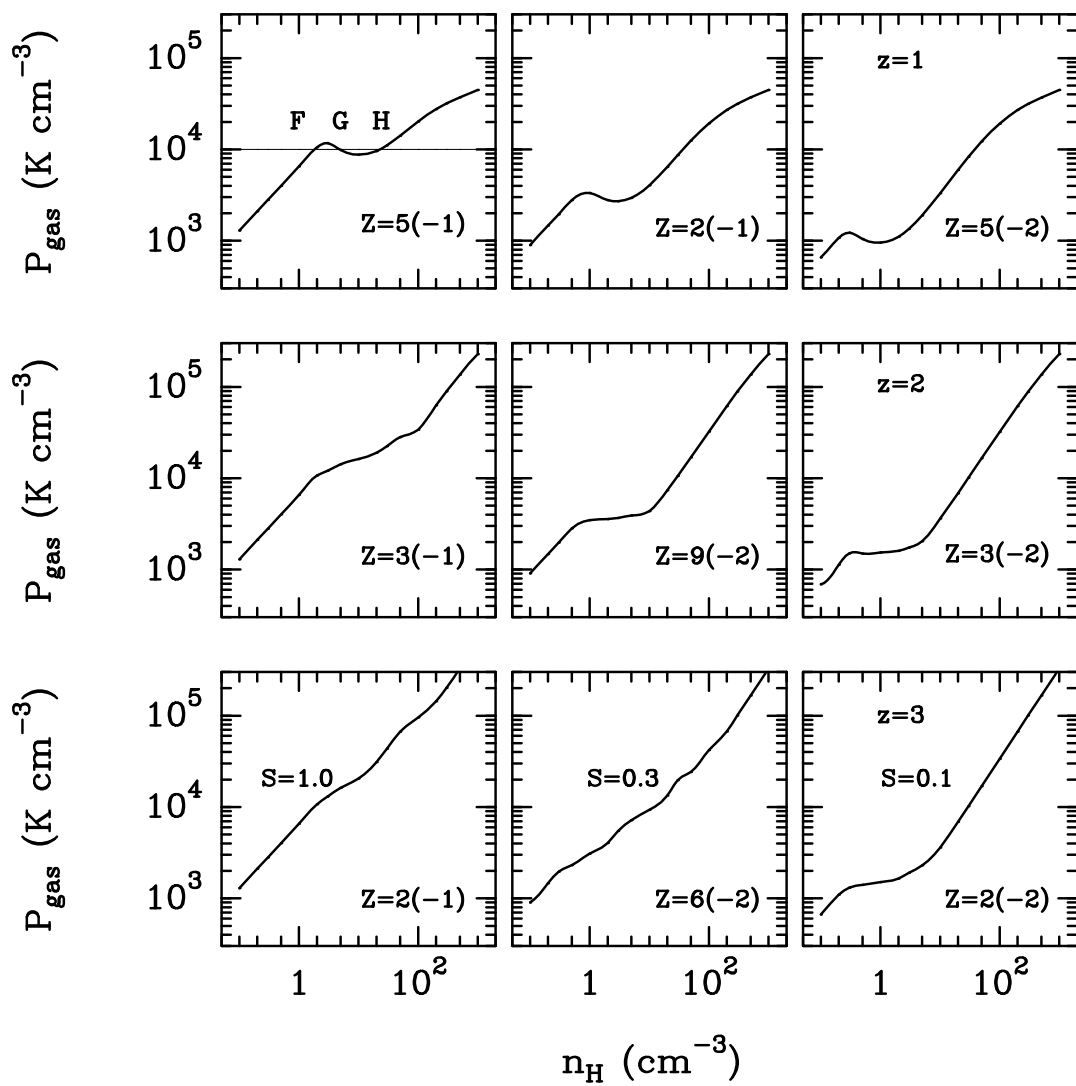


Fig. 5.—